Hindawi
Advances in Civil Engineering
Volume 2023, Article ID 1443006, 9 pages
https://doi.org/10.1155/2023/1443006

Research Article

Development and Experimental Study of a Self-Aware Posttensioned Prestressed Intelligent Reinforcement Structure

Guodong Li,[1] **Xiaotong Jing**,[1,2] **Jinbo Wang**,[1] **and Chunguang Lan**[2]

[1]*Collegue of Civil and Transportation Engineering, Northeast Forestry University, Harbin 150040, China*
[2]*Beijing Construction Engineering Research Institute Co., Ltd., Beijing 100039, China*

Correspondence should be addressed to Chunguang Lan; lcg98011210@163.com

Received 24 May 2023; Revised 2 July 2023; Accepted 21 August 2023; Published 15 September 2023

Academic Editor: Krishanu Roy

A self-aware posttensioned prestressing intelligent reinforcement system with force and sensors is proposed by combining the advantages of posttensioned prestressing reinforcement technology and intelligent structure. A static test study is then conducted with brick masonry members (wall pieces) as reinforcement objects. The experimental results demonstrate that the intelligent strand can be deployed using the same process, tensioning apparatus, and anchoring equipment as ordinary strand. Furthermore, the mechanical performance indexes with and without intelligent strands are very close, and the differences in percentages of cracking load, cracking displacement, yielding load, yielding displacement, ultimate load, and ultimate displacement are 20%, 9%, 9%, 10%, 2%, and 26%.

1. Introduction

Continuous advancements in engineering technology necessitate regular updates to building structure design and construction methods [1, 2]. The advent of innovative technologies, such as posttensioned prestressing technology [3, 4] and intelligent structures [5], has resulted in unprecedented improvements to building project design, construction, and maintenance. Not only have these technologies altered conventional notions of building and structural engineering, but they have also elevated the safety, stability, and durability of buildings and structures to new levels.

Posttensioned prestressing reinforcement technology is widely used for the retrofit of reinforced concrete and brick and mortar structures due to its advantages of short reinforcement time, low cost, and improved seismic performance [6–8]. Liu et al. [9] discussed the design calculation method for posttensioned prestressed reinforced concrete flexural members. They proposed the common arrangement of prestressing tendons and analyzed the nodal practice. Furthermore, they analyzed the construction method of prestressed reinforced frame beams using an engineering example. Ban et al. [10] introduced a novel approach for posttensioned prestressed reinforced brick masonry incorporating structural columns. The study combined experimental tests and finite-element simulations to demonstrate the effectiveness of the proposed method. Hua and Liu [11] presented a new technique for posttensioned prestressing seismic strengthening, focusing on a seismic strengthening project involving a multistory brick and mortar house in Beijing. They conducted an experimental study on eight test walls subjected to repeated horizontal low circumferential loads to assess the shear bearing capacity and enhance the damage pattern.

Based on the aforementioned findings, the application of posttensioned prestressing reinforcement technology for strengthening and retrofitting is considered justifiable and has significant potential. However, structures reinforced using posttensioning prestressing require regular manual inspection and maintenance to ensure the integrity of the anchorage system. Moreover, these structures have limited flexibility, making it challenging to implement any changes or modifications once the strengthening process is completed. In contrast, intelligent structure technology is an approach that integrates sensors, controllers, and actuators into the structure to enable self-adaptation, self-monitoring, and self-healing [12–16]. Moreover, it can help designers monitor

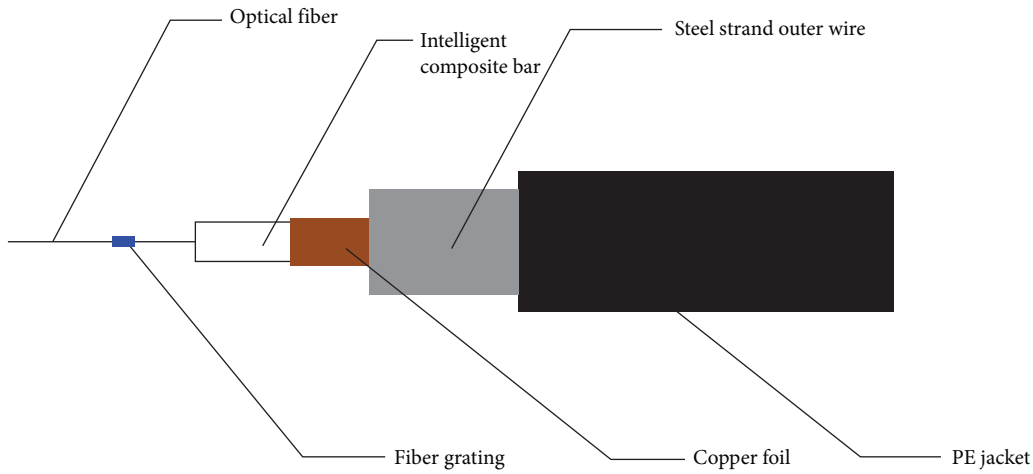

Figure 1: Schematic diagram of intelligent steel strand structure.

and control the application process of posttensioned prestressing techniques to ensure optimal results.

Based on the development and performance analysis of intelligent steel strands, this article proposes a self-aware posttensioning prestressing intelligent reinforcement system that incorporates both force and sensors. The study uses brick masonry elements (wall pieces) as the objects of reinforcement, and conducts experimental research on the self-aware posttensioned prestressing intelligent reinforcement of brick wall pieces to obtain the prestress evolution law of the reinforced structural members throughout their service life through the use of intelligent steel strands. This verifies the feasibility and superiority of the monitoring method.

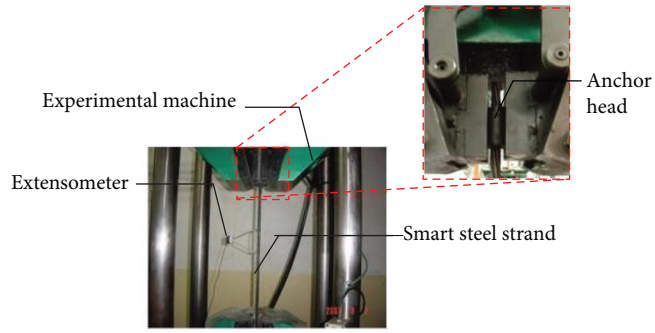

Figure 2: Photographs of the test setup.

2. Intelligent Steel Strand Search

2.1. Structure and Principle. To meet the demand for prestress loss monitoring of prestressing tendons, the intelligent strand structure must possess the following characteristics: (1) easy deployment; (2) high durability; (3) good long-term reliability; and (4) replaceability with ordinary steel strands. Our designed fiber-optic intelligent strand components include a reinforcing fiber intelligent composite tendon, copper sheet, and steel strand outer wire, which exhibit the specific structure depicted in Figure 1.

To monitor the prestress loss, we designed and manufactured the reinforced fiber-optic (FRP-BOTDA/R (FBG)) smart sensing tendon. This intelligent sensing tendon replaces the middle wire of the ordinary strand (as shown in Figure 1). The stranded end provides anchoring and torsion effects, which naturally grip and wrap the smart sensing tendon, ensuring that the six outer wires of the smart sensing tendon and the common strand deform together.

2.2. Performance Analysis

2.2.1. Mechanical Performance. The intelligent steel strand is a reinforced fiber intelligent sensing tendon that replaces the core wire of an ordinary steel strand. There are inevitably differences in mechanical properties between the two, and in order to quantify these differences, comparative tests were performed on the mechanical properties of the two strands.

The specimen length of this test is 700 mm. Since the surface of the steel strand is threaded, there is a risk of slippage between the steel strand and the tensile testing machine jaws during the tensile test, which could prevent the steel strand from reaching its tensile limit and being damaged. To prevent this, YM15 single-hole round anchor anchorage was used to grip the steel strands and anchor them into the jaws of the experimental machine for tensioning. Tensile testing was conducted using a LYE-600A testing machine with a loading speed of 3 mm/min, and the load value was recorded by the integrated pressure transducer. Strain testing was conducted using YYU-10010 strain gauges with a sampling frequency of 2 Hz during loading. Three specimens were tested, including two intelligent strands and one ordinary strand. The tension test setup for steel strands is shown in Figure 2.

2.2.2. Results and Analysis. Select specimens that meet the damage criterion requirements (as shown in Figure 3), record force transducer and extensometer readings on the tensile testing machine at all levels of loading, and create principal structure relationship diagrams and mechanical property indices for each strand, as shown in Figure 4 and

Figure 3: Intelligent steel strand breakage photo.

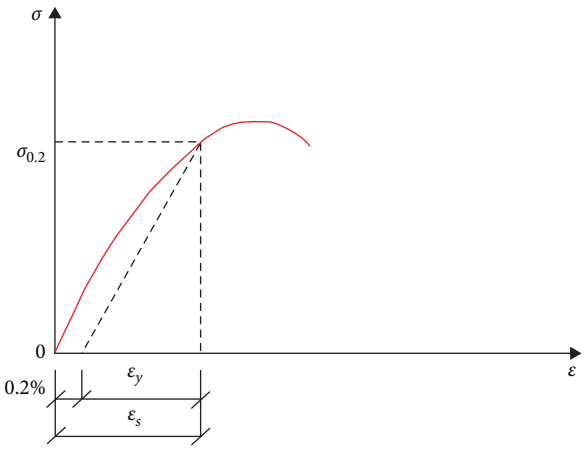

Figure 4: Stress–strain relationship curve.

Table 1: Summary of mechanical property indexes of the three specimens.

Number	Specify nonproportional extension force (kN)	Specified total extension force (kN)	Maximum force (kN)	Elasticity modulus (GPa)	Maximum force total elongation (%)	Tensile strength (MPa)
1	215.2	211.3	232.3	171.0	2.7	1,660
2	214.0	208.9	235.0	168.6	3.0	1,680
3	238.5	234.9	265.0	193.6	7.2	1,890

Table 1, respectively. Numbers 1 and 2 are intelligent steel strand and Number 3 is ordinary steel strand.

Based on the comparison of the mechanical property parameters of the intelligent and ordinary strands in Table 1, it is evident that the tensile strength of the two intelligent strands is essentially similar, surpassing 1,660 MPa, which represents approximately 88% of the tensile strength of the ordinary strand. The maximum tensile force exceeds 230 kN, and the GFRP tendons break when the strain variation exceeds 27,000 $\mu\varepsilon$.

2.2.3. Fiber Grating Sensing Performance. To verify the sensing characteristics of the fiber grating sensor in the intelligent steel strand, a calibration test was performed. A 3-meter long fiber grating intelligent strand was used as the test object, and a 300-kN jack and counterforce frame served as the testing equipment. The fiber grating wavelength demodulation was conducted with the MOI Si720 fiber grating demodulator, while a resistance-strain pressure sensor was installed between the jack and counterforce frame, as shown in Figure 5. The test was conducted in four levels of load: 50, 100, 150, and 200 kN,

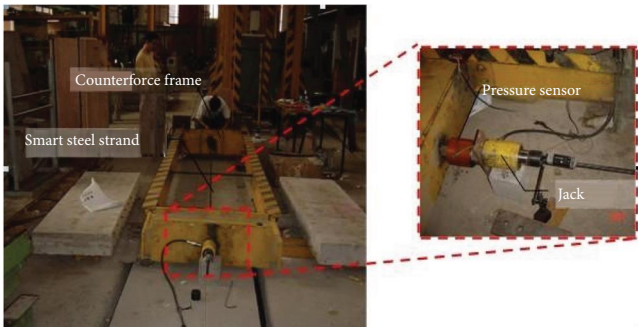

Figure 5: Photo of intelligent steel strand calibration device.

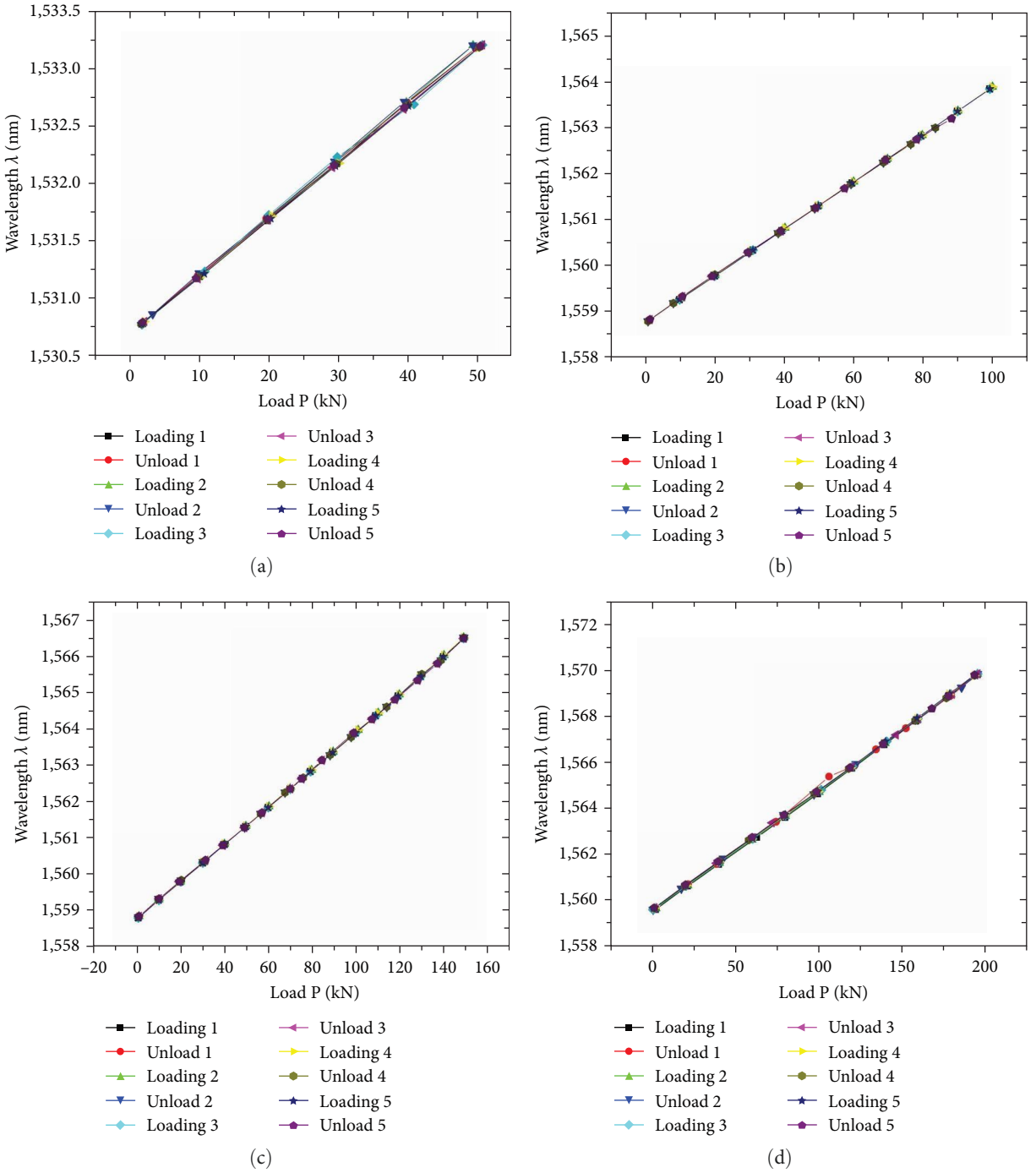

Figure 6: Results of the intelligent strand calibration test. (a) Calibration result for maximum load of 50 kN. (b) Calibration result for maximum load of 100 kN. (c) Calibration result for maximum load of 150 kN. (d) Calibration result for maximum load of 200 kN.

and each level was loaded in increments of 10 kN and then unloaded to a force-free state in the same steps. Five cycles were repeated for each stage.

2.2.4. Results and Analysis. Figure 6 illustrates the results of the calibration test, which show that the fiber grating sensor embedded in the intelligent strand possesses a wide measurement range (up to 7,000 $\mu\varepsilon$), high linearity (linear correlation coefficient of 99.99%), and excellent repeatability. The sensitivity of the intelligent strand at test loads of 50, 100, 150, and 200 kN was measured to be 50.54, 51.37, 51.79, and 52.78 pm/kN, respectively. The strain sensitivity coefficient of the intelligent strand remained constant throughout the tensile force up to 200 kN, which indicates that the outer layer of the intelligent strand steel wire and the intelligent sensing tendon work in concert. These results demonstrate the feasibility and accuracy of the test from the perspective of the working mechanism.

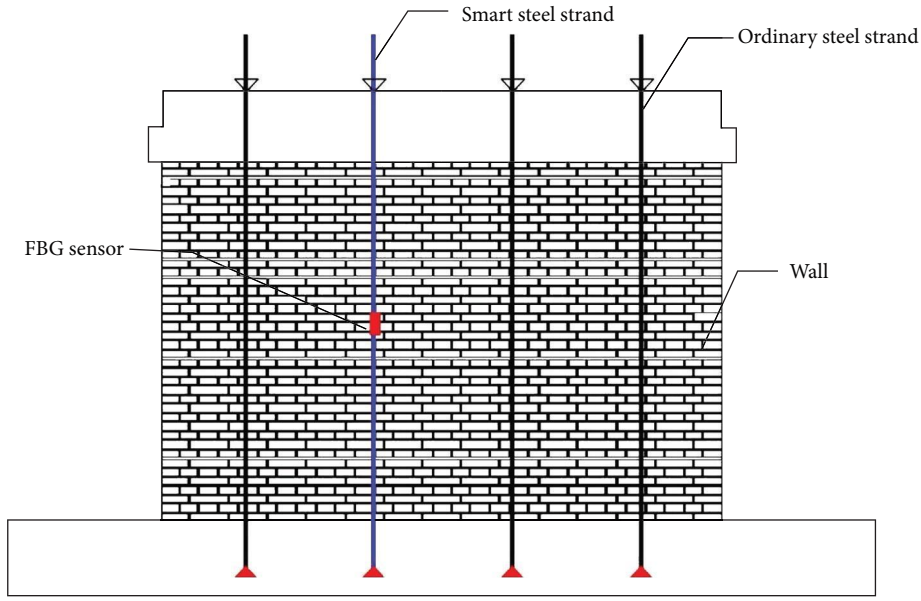

Figure 7: Schematic diagram of self-aware posttensioning prestressing intelligent reinforcement system.

3. Self-Aware Posttensioned Prestressing Intelligent Reinforcement Structure

Although the ultimate bearing capacity of the intelligent strand is about 90% of the ordinary strand, it is still acceptable since the tensioning control force during construction is approximately 70%–75% of the ultimate bearing capacity, while the effective stress retention of the strand is around 50%–60% after removing the transient loss. A slight decrease in mechanical properties does not affect the posttensioned prestressed structure. Moreover, considering the worse stress performance of existing structures, the effective stress selection for posttensioned prestressed reinforcement technology is smaller than that of the new structure. Therefore, it is possible to use intelligent strand in situ instead of ordinary steel strand for the structure. Consequently, we propose a self-aware posttensioning prestressing intelligent reinforcement structure based on fiber-optic sensing technology using intelligent steel strand, as illustrated in Figure 7.

4. Self-Aware Intelligent Wall Panels: Experimental Study

4.1. Overview of the Experiment. Specifically, static experiments were conducted on posttensioned prestressed brick masonry wall pieces. The research included five wall pieces without structural columns or windows and five wall pieces without structural columns but with windows, where two strands of each wall were replaced with new intelligent steel strands. The proposed static test is used as the experimental loading method, and the ultimate damage of the reinforced wall is the experimental termination form. The main materials of the test specimens were selected based on their popularity, as follows: (1) red bricks of size $240 \times 115 \times 53$ mm, with a MU10 grade; (2) mixed mortar of M5 grade; (3) fine stone concrete of C20 grade for the ring beam and pressure top beam; (4) higher grade concrete than the ring beam and pressure top beam for the bottom beam due to the larger load it receives; (5) HPB235 grade for the longitudinal reinforcement in the beam and hoop reinforcement; (6) 1,860 grade 15.2 mm diameter seven-wire steel strand for the prestressing reinforcement; (7) Q345 structural steel for the steel members in the specimen; (8) the intelligent steel strand is encapsulated with a fiber-optic grating intelligent sensing tendon in glass fiber; and (9) a 0.02 mm brass copper foil is used to protect the sensing tendon.

Figure 8 illustrates the schematic diagram of the experimental loading device. After constructing and curing the test wall for 28 days in accordance with the relevant specifications, the wall is mounted on the testing platform using a crane and then anchored to the ground beam with anchor bolts. A vertical load equivalent to a simulated live load of 220 kN is applied to the wall using an electrohydraulic servo hydraulic jack, while a horizontal reciprocating load equivalent to a simulated earthquake is applied using a 100 tonne electrohydraulic servo jack installed on the counterforce wall.

4.2. Experimental Results and Analysis

4.2.1. Analysis of Mechanical Performance. Typically, the intelligent strand and their role in reinforced structures, they can theoretically serve as intelligent members. To verifensor may introduce structural defects to the system, but this issue can be resolved using the sensor as both a sensing element and a mechanical component. Considering the structural features of intelligent strandsy this notion, intelligent strand reinforced wall pieces were laid alongside non-intelligent strand reinforced wall pieces under similar conditions, and their mechanical properties were compared. Here, we only analyze the mechanical properties of the wall pieces without window openings. Figures 9 and 10 display photos of the damage and crack distribution in the unreinforced wall piece, the deployed intelligent stranded wall

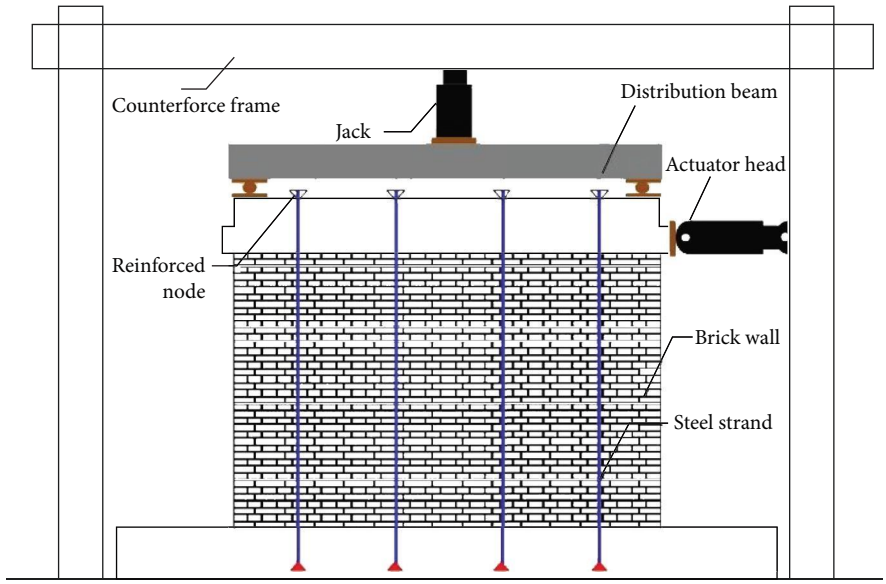

Figure 8: Schematic diagram of the test loading device.

(a) (b) (c)

Figure 9: Photos of wall damage. (a) Unreinforced wall piece. (b) Wall piece with intelligent strand. (c) Wall piece without intelligent strand.

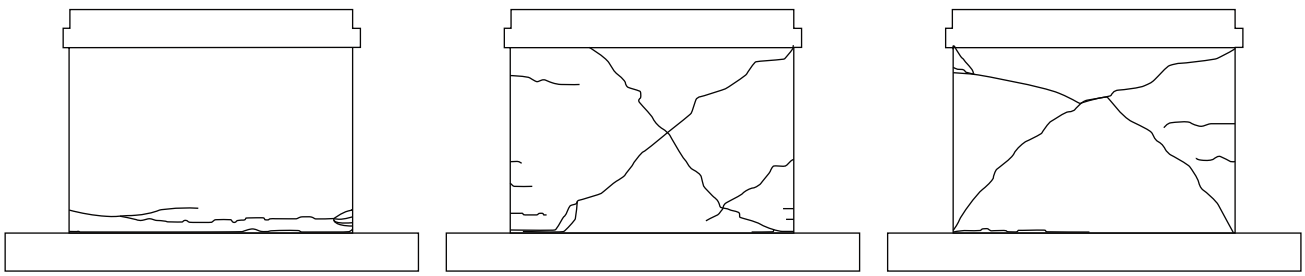

(a) (b) (c)

Figure 10: Photos of the crack distribution. (a) Unreinforced wall piece. (b) Wall piece with intelligent strand. (c) Wall piece without intelligent strand.

piece, and the unmounted intelligent stranded wall piece, respectively. In Figure 11, the hysteresis curves of the unreinforced wall pieces, the fabricated intelligent stranded wall pieces, and the unfabricated intelligent stranded wall pieces are presented.

Figure 11 illustrates that the ultimate bearing capacity, ultimate load, and energy dissipation capacity of the wall with and without intelligent strand are higher than the unreinforced wall. Further examination of the reinforced walls with and without intelligent strands shows that the ultimate bearing capacity and ultimate displacement values of the two walls are similar. Table 2 considers each of the three walls' main performance indicators. From the table, it can be seen that the mechanical performance indexes with and without the intelligent strand are very similar, and the percent differences of cracking load, cracking displacement, yield load, yield displacement, ultimate load, and ultimate displacement are 20%, 9%, 9%, 10%, 2%, and 26%, respectively. The above

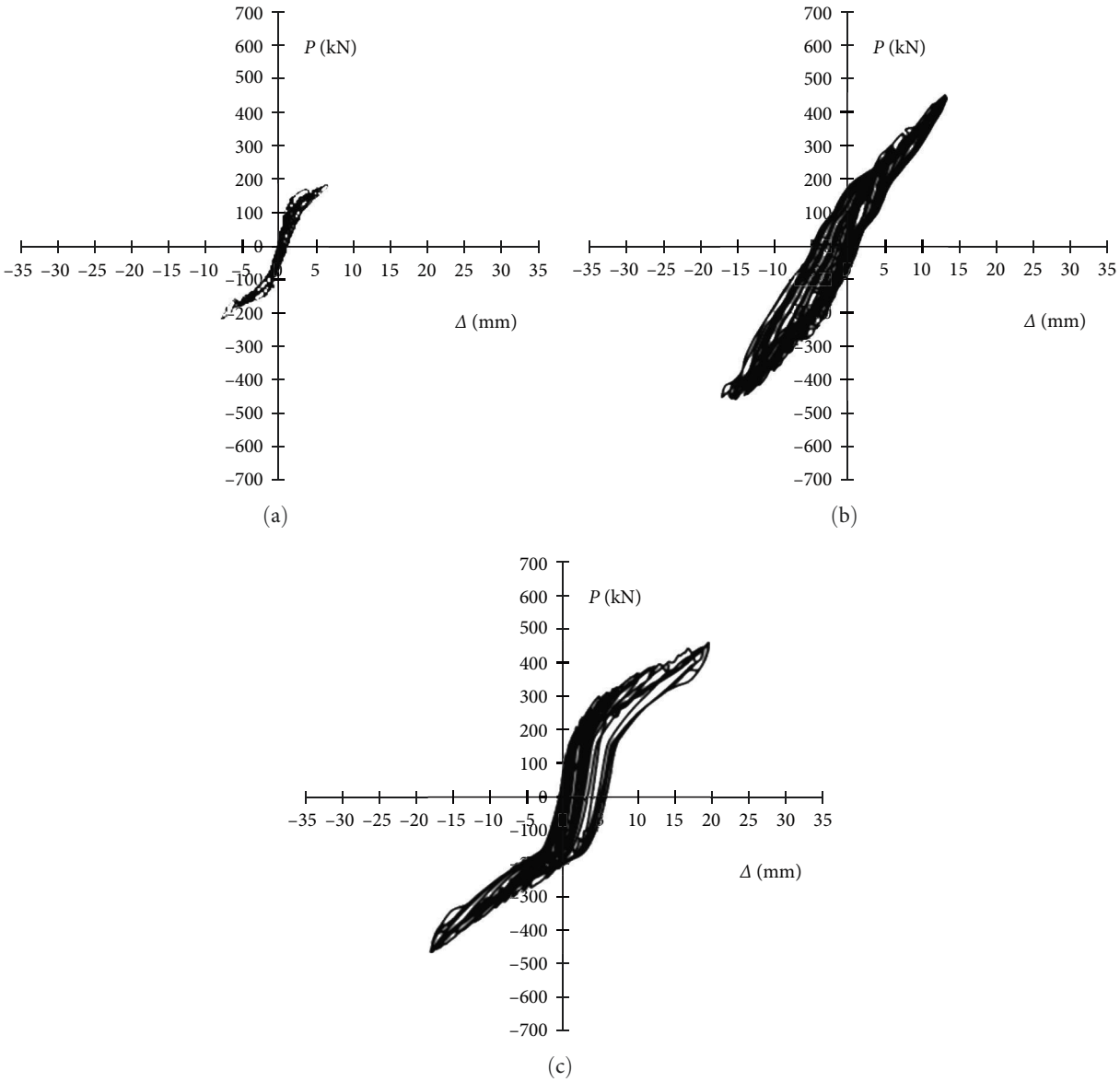

Figure 11: Comparison of hysteresis curves with and without self-aware steel stranded wall pieces. (a) Unreinforced wall piece. (b) Wall piece with intelligent strand. (c) Wall piece without intelligent strand.

Table 2: Key mechanical property indices of the three types of walls.

Number	Unreinforced wall	Reinforced walls			
		Nonintelligent steel strand	With intelligent steel strand	Difference	Percentage (%)
Cracking load (kN)	75	100	120	20	20
Cracking displacement (mm)	0.6	0.98	0.89	−0.09	9
Yield load (kN)	152	280	255	−25	9
Yield displacement (mm)	2.8	5	4.5	−0.5	10
Ultimate load (kN)	195	444	451	7	2
Ultimate displacement (mm)	6.85	14.8	18.6	3.8	26

indicators, except for cracking load and ultimate displacement, are all very close to each other. Considering that the experimental process adopts force control and manual methods are used to identify cracks and determine the cracking load, the accuracy of the cracking load value is compromised due to suboptimal lighting conditions in the laboratory. Moreover, small cracks in the brick masonry wall are easily overlooked. Therefore, the determination of the cracking

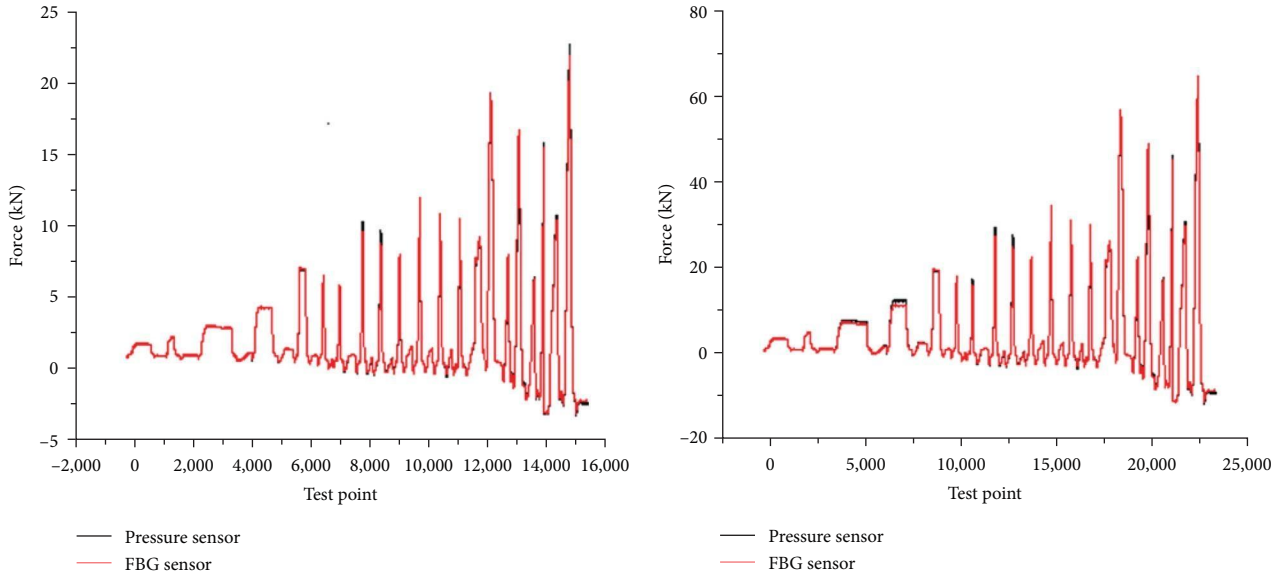

FIGURE 12: Comparison of self-aware steel strands and traditional test methods for the entire static experiment process. (a) Windowless wall. (b) Wall with window cavity.

load value is not highly precise. Additionally, the brick masonry wall itself exhibits significant discreteness. Hence, these comparative mechanical performance indicators can demonstrate the minimal impact of deploying smart steel strands on the mechanical properties of the reinforced wall.

4.2.2. Analysis of Sensing Performance. To verify the test results of the intelligent strand, a penetration-type resistance-strain pressure sensor was installed between the anchor head and anchor pad of the intelligent strand. The dynamic acquisition of the whole experiment was carried out using the same sampling frequency as the fiber grating sensor inside the intelligent strand. Figure 12 shows the experimental results of posttensioned prestressing reinforced wall pieces with and without window cavit.

As shown in Figure 12, the fiber grating sensor's test results within the intelligent strand match well with those of the penetration type mechanics sensor. Examining the numerical changes reveals that the maximum error between the intelligent steel strand and the mechanical sensor test results is less than 10% for both the wall without a window cavity and the wall with a window cavity. This demonstrates the accuracy and feasibility of using the intelligent steel strand to monitor the change in prestress force value of the posttensioned prestressed reinforced brick wall.

5. Conclusions

(1) The intelligent strand can use the same laying process, tensioning apparatus, and anchoring equipment as ordinary strands, making construction simple and convenient. The fiber-optic sensor within the intelligent strand can accurately monitor the stress evolution of the posttensioned prestressing tendons in existing reinforced structural members at all stages, allowing for the effective prestress value to be obtained.

(2) The percent difference between the walls with intelligent strands and those with ordinary strands were 20% for cracking load, 9% for cracking displacement, 9% for yield load, 10% for yield displacement, 2% for ultimate load, and 26% for ultimate displacement. Notably, the walls equipped with intelligent strands had higher cracking load and ultimate displacement values than those with ordinary strands.

(3) The maximum error of the test results obtained from both the fiber grating sensor and the pressure sensor inside the intelligent strand is less than 10%, thus verifying the superiority and effectiveness of the monitoring performance of the intelligent reinforced structure.

Data Availability

Data available on request from the authors. The data that support the findings of this study are available from the corresponding author (Chunguang Lan), upon reasonable request.

Conflicts of Interest

The authors declare that they have no conflicts of interest.

Acknowledgments

Project of Beijing Natural Science Foundation, Development and application of self-aware and self-diagnostic posttensioned prestressing intelligent reinforcement system (Grant Number 8192017), 2018.

References

[1] C. W. Hu, "Structural design and construction recommendations for multi-story buildings with prestressed concrete truss transition floors," *Urban Architecture*, no. 33, pp. 61–61, 2016.

[2] Y. Q. Zhou, "Exploring the core of the application of structural design and construction technology of masonry buildings," Chinese Master's Theses Full-text Database, (7):0094-0096, 2022.

[3] J. Kraľovanec, M. Moravčík, P. Bujňáková, and J. Jošt, "Indirect determination of residual prestressing force in post-tensioned concrete beam," *Materials*, vol. 14, no. 6, Article ID 1338, 2021.

[4] S.-H. Kim, S. Y. Park, and S.-J. Jeon, "Long-term characteristics of prestressing force in post-tensioned structures measured using smart strands," *Applied Sciences*, vol. 10, no. 12, Article ID 4084, 2020.

[5] J. Xie, B. Gao, and H. Cheng, "Research and development of civil engineering intelligent structure system," *Advances in Civil Engineering*, vol. 2021, Article ID 8814676, 10 pages, 2021.

[6] C. G. Lan, L. R. Ban, M. J. Han, and H. Liu, "Seismic behavior of no structural column clay brick walls retrofitted by post-tensioned tendons," *Earthquake Engineering and Engineering Dynamics*, vol. S1, pp. 560–565, 2014.

[7] M. Turan, "A case study on two-span post-tensioned concrete bridge decks with different span lengths and investigation on prestressing tendons with comparisons," *Sakarya University Journal of Science*, vol. 24, no. 4, pp. 575–585, 2020.

[8] N. Ismail and J. M. Ingham, "Time-dependent prestress losses in historic clay brick masonry walls seismically strengthened using unbonded posttensioning," *Journal of Materials in Civil Engineering*, vol. 25, no. 6, pp. 718–725, 2013.

[9] H. Liu, H. Z. Gao, and X. Z. Yang, "Post-tensioned extracorporeal prestressing reinforcement technology and its engineering application," *Construction Technology*, vol. 43, no. 1, pp. 49–52, 2012.

[10] L. R. Ban, H. Liu, C. Z. Qi, S. F. Hua, Y. Gong, and Y. D. Xue, "Research on the properties of brick walls with structural concrete columns retrofitted by post-tensioned tendons," *Industrial Construction*, no. 11, pp. 95–99, 2017.

[11] S. F. Hua and H. Liu, "Research and application of post-tensioned prestressing reinforcement technology for a multi-story brick house," *Building Structure*, vol. 43, no. S1, pp. 1412–1416, 2013.

[12] X. X. Chen, "Investigation and research on the current situation of primary and junior high school bridging courses in nine-year consistent school," Chinese Master's Theses Full-text Database, 25-28.2022

[13] J. P. Ou and X. C. Guan, "Research and development of intelligent structural system for civil engineering," *Earthquake Engineering and Engineering Vibration*, vol. 19, no. 2, pp. 21–28, 1999.

[14] X. B. Gong, "Research and development of intelligent structural system for civil engineering," *Industry and Technology Forum*, no. 5, pp. 57-58, 2020.

[15] W. G. Xie, "Research and development of intelligent structural system for civil engineering," *Journal of Jiamusi Vocational College*, vol. 36, no. 5, pp. 253-254, 2020.

[16] L. F. Long, "Analysis of the current status and applications of intelligent civil engineering research," *Industrial Innovation*, no. 2, pp. 117–119, 2023.